DOI 10.5012/bkcs.2011.32.2.536

The Origin of the Residual Carbon in $LiFePO_4$ Synthesized by Wet Milling

Sung Bin Park, Chang Kyoo Park, Jin Tae Hwang, Won Il Cho,† and Ho Jang*

*Department of Materials Science and Engineering, Korea University, Seoul 136-701, Korea. *E-mail: hojang@korea.ac.kr*
†Battery Research Center, Korea Institute of Science and Technology 39-1, Hawolgok-dong, Seongbuk-gu, Seoul 136-791, Korea
Received October 8, 2010, Accepted December 6, 2010

This study reports the origin of the electrochemical improvement of $LiFePO_4$ when synthesized by wet milling using acetone without conventional carbon coating. The wet milled $LiFePO_4$ delivers 149 $mAhg^{-1}$ at 0.1 C, which is comparable to carbon coated $LiFePO_4$ and approximately 74% higher than that of dry milled $LiFePO_4$, suggesting that the wet milling process can increase the capacity in addition to conventional carbon coating methods. UV spectroscopy, elemental microanalysis, and evolved gas analysis are used to find the root cause of the capacity improvement during the mechanochemical reaction in acetone. The analytical results show that the improvement is attributed to the conductive residual carbon on the surface of the wet milled $LiFePO_4$ particles, which is produced by the reaction of $FeC_2O_4 \cdot 2H_2O$ with acetone during wet milling through oxygen deficiency in the precursor.

Key Words: Lithium iron phosphate, Wet milling, Mechanochemical reaction, Rate capability, Carbon coating

Introduction

Lithium-ion batteries using an olivine-type lithium iron phosphate ($LiFePO_4$) cathode have attracted much attention as a power source for electric and hybrid electric vehicles due to its low material cost, non toxicity, and better thermal stability.[1-3] However, the commercial application of $LiFePO_4$ as a cathode for lithium secondary batteries has been limited because of its low electrical conductivity and poor rate capability. Recent research efforts have focused on improving the electrical conductivity of $LiFePO_4$ by coating carbonaceous conductors[4-6] and doping with metallic elements such as Cr, Mg, Ni, or Co.[7-9]

Ravet *et al*.[4] coated $LiFePO_4$ using sucrose, cellulose acetate, and a modified polycyclic aromatic and achieved the initial discharge capacity up to 140 $mAhg^{-1}$. Prosini *et al*.[5] investigated $LiFePO_4$ coated with 10 wt % carbon black and obtained initial capacity up to 120 $mAhg^{-1}$. Chung *et al*.[7] reported that electrical conductivity of $LiFePO_4$ was enhanced by metal doping and the doped cathode delivered 140 $mAhg^{-1}$ at 0.1 C. Wang *et al.*[9] also reported the enhancement of rate performance of $LiFePO_4$ by metal doping without increasing the initial capacity. They suggested that the initial capacity is mainly improved by increasing the electrical conductivity of the $LiFePO_4$, while the rate performance could be enhanced by metal doping. On the other hand, it was also suggested that the electrical conductivity of $LiFePO_4$ could be improved by the presence of residual carbon after synthesis.[10-13] Meligrana *et al*.[13] found that residual carbon can be obtained after mild hydrothermal synthesis employing hexadecyltrimethylammonium bromide (CTAB). It would, therefore, seem that the initial capacity of the $LiFePO_4$ could be improved without rigorous carbon coating, if the mechanochemical reaction could produce carbonaceous by-products during the wet milling process. However, there is no detailed investigation about the possible formation of the carbonaceous products during wet milling and their effects on the electrochemical properties of the $LiFePO_4$.

This study focused on the root cause of the enhancement of rate performance and initial capacity of $LiFePO_4$ when acetone was used for the homogeneous mixing during milling. Evolved gas analysis (EGA), elemental microanalysis, and UV spectroscopy were employed to investigate the mechanochemical reaction of the precursors with acetone, which produced the carbonaceous byproducts and improved the electrochemical response during chage-dischage of the lithium secondary batteries.

Experimental Details

The mixture of Li_2CO_3 (Aldrich, ≥99%), $FeC_2O_4 \cdot 2H_2O$ (Aldrich, ≥99%), and $(NH_4)H_2PO_4$ (Aldrich, ≥99%) was placed in a zirconia bowl with the molar ratio of 1:2:2 and mechanochemical reaction was carried out for 3 hours using a planetary mill (FRITSCH Pulverisette 5) with a ball-to-powder weight ratio of 20:1. The rotating speed was set at 250 rpm for dry milling and 400 rpm for wet milling to compensate the damping effect from acetone. 400 rpm for dry milling showed the segregation of starting materials, 250 rpm for wet milling showed low crystallinity of $LiFePO_4$. The mixture obtained from planetary milling was heat treated at 600 ^oC using a tube furnace for 10 h under Ar +5% H_2 atmosphere. Evolved gas analysis (EGA; Py-2020iD, Frontier lab, Japan, and 6890N GC/5975i MS, Agilent, USA) was carried out to examine the gaseous products during the heat treatment. The wet milling media after the milling process was analyzed by an ultraviolet-visible spectrophotometer (UV: S-3100, Scinco, Korea). For UV analysis, each starting material was milled in acetone at the same condition as $LiFePO_4$ and the acetone was retrieved after milling to analyze using UV spectroscopy.

The crystal structure of $LiFePO_4$ was examined by X-ray diffraction (XRD; D/MAX-II A) with Cu Kα in a scan range of

2θ: 15 ~ 45°. The lattice parameter was calculated by UnitCell software.[14] The morphology of the $LiFePO_4$ was examined by a field emission scanning electron microscope (FE-SEM, Hitachi, S-4300, Japan) and TEM (JEOL, JEM-2100F, Japan). TEM specimen was prepared by dropping a dilute ethanol solution containing $LiFePO_4$ particles on a Cu grid. The amount of residual carbon in the $LiFePO_4$ was measured by elemental analyzer (ThermoFinnigan, Flash EA 1112, Italy).

The cathodes were prepared by slurring the active material with 5 wt % polyvinylidene fluoride and 10 wt % acetylene black (w/w) in an n-methyl pyrrolidone solvent. The mixture was coated onto an Al foil and dried at 80 °C in a ventilation oven. After drying, the cathodes were held in a vacuum oven at 80 °C for 12 h. The cathode was 60 μm thick and contained approximately 5 ~ 7 mg cm^{-2} of the active material. The charge and discharge characteristics of the cathode were examined using a coin cell (2032 type). The electrolyte was 1M $LiPF_6$ in an ethylene carbonate/dimethyl carbonate/ethylmethyl carbonate solution and a lithium foil was used as a counter electrode. The galvanostatic charge-discharge experiment was performed using a Maccor 4000 battery cycler with cut-off voltages in the range of 2.5 - 4.3 V.

Results and Discussion

The structure and average particle size of wet and dry milled $LiFePO_4$ were examined using XRD since they can strongly affect the electrochemical performance during charge and discharge cycles. Fig. 1 shows XRD patterns obtained from the $LiFePO_4$ particles after the heat treatment at 600 °C. Both patterns showed typical diffraction peaks corresponding to $LiFePO_4$.[15] The lattice parameters calculated from the XRD patterns were same regardless of the milling condition (Table 1). The particle sizes of both specimens were calculated from the full-width at half maximum (FWHM) of the diffraction peaks in Fig. 1. The average sizes (D) of the wet and dry milled $LiFePO_4$ crystallites were 40.55 nm and 40.48 nm, respectively, which was estimated from the Scherrer's formula described by: $D = 0.9\lambda / \beta \cos\theta$, where $\lambda = 1.5418$ Å (Cu Kα) and β is FWHM at the diffraction angle of θ.

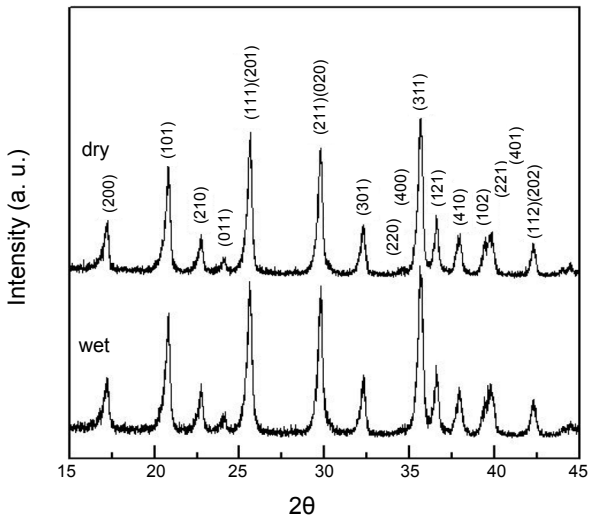

Figure 1. XRD patterns of wet milled and dry milled $LiFePO_4$.

The $LiFePO_4$ particles produced from wet and dry milling were also examined using SEM to confirm particle size distribution and to study possible byproducts produced during synthesis. Fig. 2 shows secondary electron images of (a) wet and (b) dry milled $LiFePO_4$ particles. Particle surfaces were clean when dry milling was carried out without a milling agent, while clusters of small particles were observed on the surface when the acetone was used as a milling agent. The adherent particles on the surface of the wet milled $LiFePO_4$ seemed to be attributed to the milling agent (acetone) during wet milling at a higher rotating speed (400 rpm). This is because the fast rotating speed provides high energy to accelerate the mechanochemical reaction of acetone with starting materials, which can induce the formation of new reaction products.

The same $LiFePO_4$ particles were also investigated by TEM at higher magnifications to analyze the adherent particles. Fig. 3 shows TEM micrographs of $LiFePO_4$ particles produced from wet and dry milled $LiFePO_4$. They showed clean surfaces with clear phase contrast when it was dry milled, while the wet milled $LiFePO_4$ showed adherent phases in the $LiFePO_4$ particles (Fig. 3). Elemental analysis was also carried out to examine carbon content in the $LiFePO_4$ particles produced by dry and wet milling processes. The results from the elementary anal-

Table 1. Lattice parameters of wet milled and dry milled $LiFePO_4$

	a (Å)	b (Å)	c (Å)
Wet milled $LiFePO_4$	10.3016	5.9939	4.6898
Dry milled $LiFePO_4$	10.3121	5.9927	4.6830

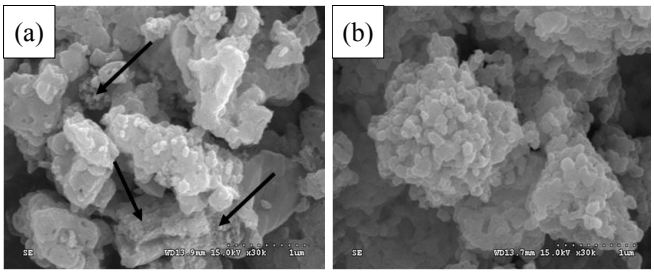

Figure 2. SEM images of (a) wet milled and (b) dry milled $LiFePO_4$.

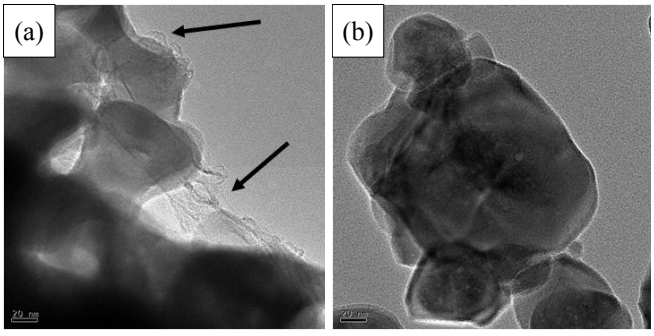

Figure 3. High resolution TEM images of (a) wet milled and (b) dry milled $LiFePO_4$.

ysis showed that carbon content of particles from wet milling was approximately 4 times greater than that from dry milling (Table 2).

Using the wet and dry milled $LiFePO_4$, the initial capacity during discharge was measured to examine the possible effects of acetone on electrochemical performance. Fig. 4 shows the specific capacity of dry and wet milled $LiFePO_4$ up to 50 cycles. The initial capacity of the dry milled $LiFePO_4$ delivered 68 $mAhg^{-1}$ at 0.2 C, which was similar to that of bare $LiFePO_4$.[16-18] On the other hand, wet milled $LiFePO_4$ delivered much improved initial capacity of 143 $mAhg^{-1}$ at 0.2 C and this was comparable to the carbon-coated $LiFePO_4$.[19-21] This suggests that the carbonaceous product produced on the particle surface during wet milling plays a similar role as the conductive layer from the conventional carbon coating $LiFePO_4$. The initial capacity of $LiFePO_4$ improved by carbon coating has been reported by others and they are compared in the Table 3. The table indicates that the carbon layer on the particle surface, which was produced by wet milling, increases electrical conductivity of $LiFePO_4$ and initial capacity. Fig. 4 also indicated that the wet milled $LiFePO_4$ retained 99% of the initial capacity after 50 cycles at 0.2 C, whereas the dry milled $LiFePO_4$ showed only 88% capacity retention. It suggested that the residual carbon from wet milled precursor not only enhanced the capacity of $LiFePO_4$ but also improved cyclability. Although the amount of residual carbon was smaller than the carbon coated by other conventional methods, it was noteworthy to find a similar level of capacity retention.

Several researches have been carried out conventional carbon coating by using milling agents. Dong *et al*.[23] reported carbon coated $LiFePO_4$ delivering 156 $mAhg^{-1}$ of the initial capacity by using acetone as a milling agent. Yang *et al*.[24] reported 158 $mAhg^{-1}$ of initial capacity for $LiFePO_4$/polyacenes milled with ethanol. Zhang *et al*.[25] reported carbon coated $LiFePO_4$ with ethanol by using conventional carbon coating method. Initial capacity of $LiFePO_4$ was 145.5 $mAhg^{-1}$ at 0.5 C which was similar value compared to our experiment. These experiments also could be affected by the residual carbon effect due to the milling agent. We also have synthesized the $LiFePO_4$ with acetone, ethanol, and methanol without additive carbon sources. Electrochemical performances of those samples showed similar values suggesting residual carbon was obtained by the milling agents.

The capacity of dry and wet milled $LiFePO_4$ was compared to examine their cyclability at high C rates. Fig. 5 shows the specific capacity when the charge-discharge rate is increased from 0.1 to 20 C. At 5 C, the capacity of the dry milled $LiFePO_4$ delivered almost no current, while wet milled $LiFePO_4$ maintained arpproximately 50% of the initial capacity (75 $mAhg^{-1}$). The poor charge-discharge performance of the dry milled $LiFePO_4$ at high C rates is attributed to high electrical resistance and high polarization. However, both specimens showed almost no current at higher charge-discharge rates over 10 C. This indicated that the residual carbon on the particle surface from wet milling was not sufficient to sustain the cyclability over 10 C, suggesting further treatments such as a doping with metallic elements was needed to retain good performance at high C rates. Fey *et al*.[26] also reported the similar capacity degradation of carbon coated $LiFePO_4$ at high C rates.

The charge-discharge characteristics of the wet and dry milled $LiFePO_4$ were also examined (Fig. 6). This is because the length of the plateau indicates the operation capacity, with a longer plateau being of great advantage for a longer cell operation. The figure showed that the wet milled $LiFePO_4$ exhibited a longer plateau than that of the dry milled $LiFePO_4$, indicating that the wet milled $LiFePO_4$ delivered more capacity. It also indicated that the wet milled $LiFePO_4$ was charged at lower voltage than that of the dry milled $LiFePO_4$. This is another evidence for enhancing the electrical conductivity of wet milled $LiFePO_4$ since low voltage is needed to produce a constant current when charging.

In order to find the source of the extra carbon in the $LiFePO_4$ particle produced after wet milling, evolved gas analysis was carried out using the wet and dry milled precursors before heat-treatment (Fig. 7). The different profiles in the figure indicated that the precursors had dissimilar chemical states after wet or

Table 2. The amount of carbon in $LiFePO_4$

Materials	Wet milling	Dry milling
Carbon (wt %)	2.08	0.47

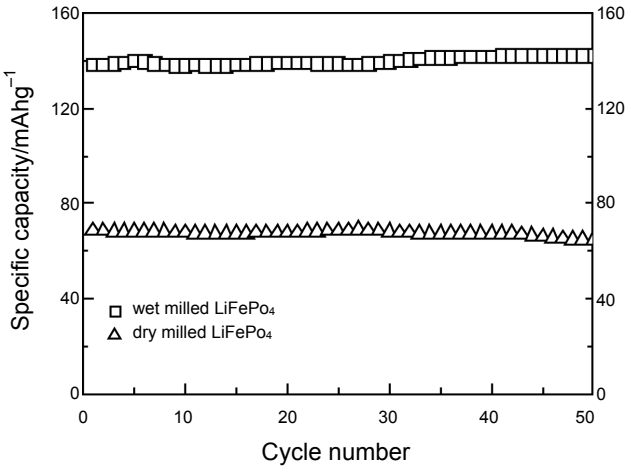

Figure 4. Cycle performance of wet and dry milled $LiFePO_4$.

Table 3. Comparison of initial capacity at 0.1 C

Materials	Graphite 0.1C [22]	Carbon black 0.1 C [22]	Acetylene black 0.1 C [22]	Sucrose 0.143 C [12]	Wet 0.1 C	Dry 0.1 C
Initial capacity ($mAhg^{-1}$)	141	140	138	120	143.48	82.24

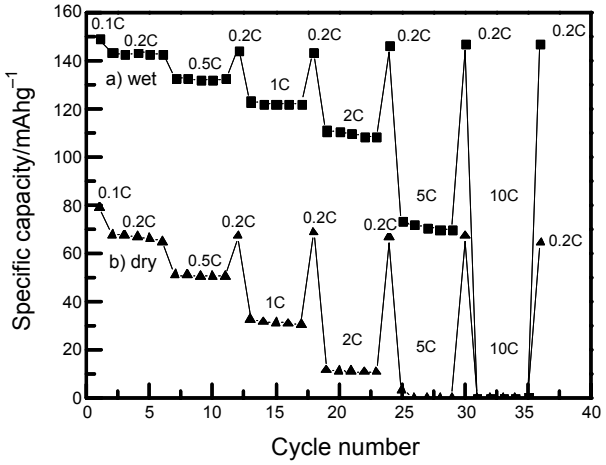

Figure 5. Rate performances of (a) wet and (b) dry milled $LiFePO_4$.

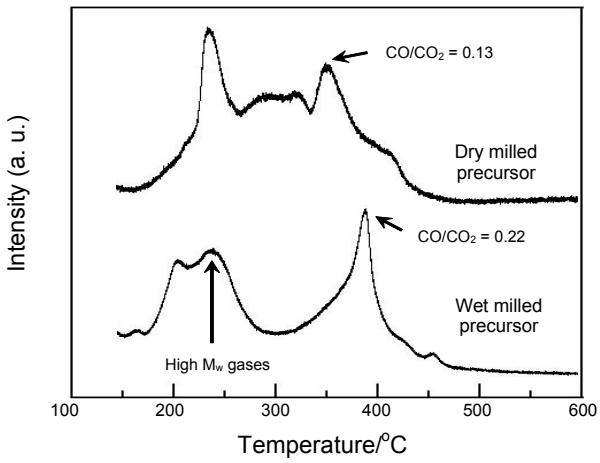

Figure 7. EGA analysis of wet milled and dry milled $LiFePO_4$.

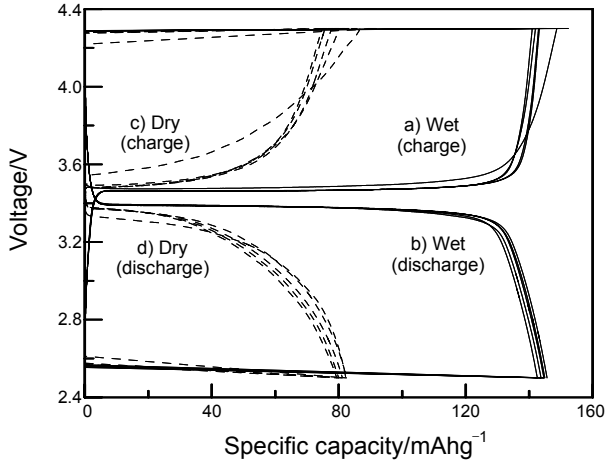

Figure 6. Charge-discharge characteristics of wet milled (solid line) and dry milled (dashed line) $LiFePO_4$.

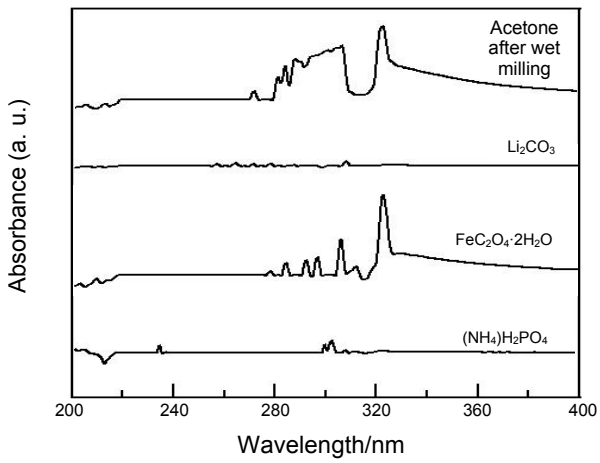

Figure 8. UV spectra of dissolved starting materials and $LiFePO_4$.

dry milling. The analysis of the evolved gas showed that the main gaseous species were CO and CO_2 and their ratio was higher ($CO/CO_2 = 0.22$) in the case of wet milled precursors than dry precursors ($CO/CO_2 = 0.13$). This indicates that the wet milled precursors generated more CO gas since it contains less oxygen. The oxygen deficiency in the wet milled precursor induced the formation of residual carbon during heat treatments since the carbon atoms in the precursor molecules were not removed as gases. In particular, the profiles from wet milled precursor exhibited a peak near 220 °C, which was consisted of high molecular weight gases ($M_w \approx 120$), suggesting possible reaction products produced by the reaction of acetone with the precursors. The amount of residual carbon as changing the acetone content was not investigated. However, since the amount of residual carbon was determined by starting materials contents, the increment of the acetone content would not affect on the residual carbon content unless too small amount of acetone was used.

In order to find the possible precursors that could be reacted by the acetone during wet milling, UV spectroscopy was employed. The spectrum of the acetone after milling the precursor showed intensity peaks in the range of wavelength between

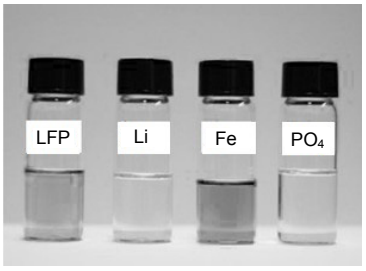

Figure 9. Acetone milled with each starting material.

270 - 320 nm (Fig. 8). The UV spectrum obtained from the acetone milled with $FeC_2O_4 \cdot 2H_2O$ showed peaks similar to those from the acetone after milling the three precursors. On the other hand, Li_2CO_3 and $(NH_4)\ H_2PO_4$ showed relatively small peaks in their spectra, suggesting that the major peaks in the spectra obtained from acetone after wet milling were mainly originated from the reaction of $FeC_2O_4 \cdot 2H_2O$ with acetone. As shown in the Fig. 9, the color of the acetone after milling with precursors also indicated that the main reaction with acetone was done by the precursor for an iron source, indicating that the high mole-

cular weight gas evolved at 220 °C during EGA analysis of the wet milled precursor is attributed to the reaction product of $FeC_2O_4 \cdot 2H_2O$ with acetone, which induced oxygen deficiency and followed by the formation of carbonaceous material during heat treatment. The further studies were needed to investigate the exact reaction product and the reaction mechanism between $FeC_2O_4 \cdot 2H_2O$ and acetone. This is a salient result because the carbonaceous byproducts produced during the mechanochemical reaction with a milling agent can play a crucial role compared to other modifications performed to improve electrochemical properties of $LiFePO_4$.

Conclusions

Wet and dry milled $LiFePO_4$ were prepared to compare their electrochemical properties without conventional carbon coating. Despite the use of the same starting materials for the $LiFePO_4$ synthesis, the morphology and electrochemical properties were different due to the acetone used for wet milling. Residual carbon was found on the surface of the wet milled $LiFePO_4$ particles, which was originated from oxygen deficiency in the precursor. The oxygen deficiency was attributed to the reaction of $FeC_2O_4 \cdot 2H_2O$ with acetone during wet milling and it induced the formation of carbonaceous materials on the particle surface. Initial capacity of wet milled $LiFePO_4$ was about 149 $mAhg^{-1}$ which was comparable to the capacity obtained from other carbon coated $LiFePO_4$. Rate capability of wet milled $LiFePO_4$ was 75 $mAhg^{-1}$ at 5 C, while dry milled $LiFePO_4$ delivered almost no current, suggesting that the residual carbon, produced by reaction of acetone with precursor, was attributed to the capcity enhancement.

Acknowledgments. This work was financially supported by a grant from the Korean Ministry of Knowledge Economy (Research grant code #: 2008EEL11P0800002009).

References

1. Padhi, A. K.; Nanjundaswamy, K. S.; Goodenough, J. B. *J. Electrochem. Soc.* **1997**, *144*, 1188.
2. MacNeil, D. D.; Lu, Z.; Chen, Z.; Dahn, J. R. *J. Power Sources* **2002**, *108*, 8.
3. Takshashi, M.; Tobishima, S. I.; Takei, K.; Sakurai, Y. *Solid State Ion*. **2002**, *148*, 283.
4. Ravet, N.; Chouinard, Y.; Magnan, J. F.; Besner, S.; Gauthier, M.; Armand, M. *J. Power Sources* **2001**, *97/98*, 503.
5. Prosini, P. P.; Zane, D.; Pasquali, M. *Electrochim. Acta* **2001**, *46*, 3517.
6. Chen, Z.; Dahn, J. R. *J. Electrochem. Soc.* **2002**, *149*, A1184.
7. Chung, S. Y.; Bloking, J. T.; Chiang Y. M. *Nat. Mater.* **2002**, *1*, 123.
8. Shi, S.; Liu, L.; Ouyang, C.; Wang, D. S.; Wang, Z.; Chen, L.; Huang, X. *Phys. Rev. B* **2003**, *68*, 195108.
9. Wang, D.; Li, H.; Shi, S.; Huang, X.; Chen, L. *Electrochim. Acta* **2005**, *50*, 2955.
10. Spong, A.; Vitins, G.; Owen, J. R. *J. Electrochem. Soc.* **2005**, *152*, A2376.
11. Konarova, M.; Taniguchi, I. *J. Power Sources* **2010**, *195*, 3661.
12. Zhang, D.; Cai, R.; Zhou, Y.; Shao, Z.; Liao, X.; Ma, Z. *Electrochim. Acta* **2010**, *55*, 2653.
13. Meilgrana, G.; Gerbaldi, C.; Tuel, A.; Bodardo, S.; Penazzi, N. *J. Power Sources* **2006**, *160*, 516.
14. Holland, T.; Redfern, S. *Mineral. Mag.* **1997**, *61*, 65.
15. Mi, C. H.; Zhao, X. B.; Cao, G. S.; Tu, J. P. *J. Electrochem. Soc.* **2005**, *152*, A483.
16. Cao, Y. L.; Yu, L. H.; Li, T.; Ai, X. P.; Yang, H. X. *J. Power Sources* **2007**, *172*, 913.
17. Yang, S. T.; Zhao, N. H.; Dong, H. Y.; Yang, J. X.; Yue, H. Y. *Electrochim. Acta* **2005**, *51*, 166.
18. Myung, S. T.; Komaba, S.; Hirosaki, N.; Yashiro, H.; Kumagai, N. *Electrochim. Acta* **2004**, *49*, 4213.
19. Kwon, S. J.; Kim, C. W.; Jeong, W. T.; Lee, K. S. *J. Power Sources* **2004**, *137*, 93.
20. Wang, G. X.; Yang, L.; Bewlay, S. L.; Chen, Y.; Liu, H. K.; Ahn, J. H. *J. Power Sources* **2005**, *146*, 521.
21. Huang, H.; Yin, S. C.; Nazar, L. F. *Electrochem. Solid State Lett.* **2001**, *4*, A170.
22. Shin, H. C.; Cho, W. I.; Jang, H. *Electrochim. Acta* **2006**, *52*, 1472.
23. Dong, Y. Z.; Zhao, Y. M.; Duan, H.; Chen, L.; He, Z. F.; Chen, Y. H. *J. Solid State Electrochemistry* **2010**, *14*, 131.
24. Yang, G.; Zhang, X.; Liu, J.; He, X.; Wang, J.; Xie, H.; Wang, R. *J. Power Sources* **2010**, *195*, 1211.
25. Zhang, L.; Peng, G.; Yang, X.; Zhang, P. *Vacuum* **2010**, *84*, 1319.
26. Fey, G. T.; Chen, Y. G.; Kao, H. M. *J. Power Sources* **2009**, *189*, 169.